Published by
NIGERIAN SOCIETY OF PHYSICAL SCIENCES
Available online @ https://journal.nsps.org.ng/index.php/jnsps

J. Nig. Soc. Phys. Sci. 8 (2026) 3412

Journal of the Nigerian Society of Physical Sciences

Applications of quadrilateral finite element meshes with four-node, eight-node, and twelve-node for efficient microwave energy transfer in curved waveguides

K. Lekhana, K. T. Shivaram*

Department of Mathematics, Dayananda Sagar College of Engineering, Visvesvaraya Technological University, Bangalore, India

Abstract

This study proposes a two-dimensional higher-order finite element method for computing eigenvalues in planar and multiply connected curved domains relevant to microwave energy transfer and electromagnetic waveguide problems. A fully automated quadrilateral mesh generator implemented in MAPLE-18 is used to convert triangular finite elements into quadrilateral elements with Four-node, Eight-node, and Twelve-node so that curved boundaries can be represented with improved accuracy. The formulation combines a Galerkin finite element procedure, an automated higher-order meshing strategy, and a Gauss quadrature rule to obtain numerical solutions of Helmholtz-type eigenvalue problems. Five curved waveguide domains are considered: an annular circular domain, a circular domain with a square hole, the union of two circular disks, a circular region with two unequal holes, and an L-shaped domain with a quarter-circular curved boundary. The computed eigenvalues are compared with published numerical and analytical results. The comparisons show that increasing the element order from Four-node, Eight-node, and Twelve-node improves the accuracy of the predicted eigenvalues while reducing the number of elements required to obtain comparable convergence. The proposed method therefore provides a practical and efficient finite element framework for eigenvalue estimation in curved waveguide geometries.

DOI: 10.46481/jnsps.2026.3412

Keywords: Quadrilateral meshing, Multiply connected regions, Eigenvalue, Finite element method.

Article History:
Received: 20 March 2026
Received in revised form: 14 April 2026
Accepted for publication: 30 April 2026
Available online: 08 June 2026

Communicated by: B. J. Falaye

1. Introduction

Transformers, motors, and generators use electromagnetic processes to convert mechanical energy into electrical energy and vice versa. These processes are part of daily life, and the interactions between electrical charges can be interpreted through electromagnetic field theory. Maxwell's equations, first published in 1864, express electromagnetic fields in terms of partial differential equations (PDEs). Physical phenomena in electromagnetics, fluid mechanics, astrophysics, quantum mechanics, solid mechanics, geoscience, and heat transport can therefore be modelled using PDEs. Analytical solutions are available only for special cases; consequently, numerical discretization methods are required. Variational frameworks are commonly used for the mathematical analysis and numerical treatment of PDEs.

Accurate prediction of electromagnetic-system behaviour is crucial for the design of new applications. Bondeson *et al.* [1] provided a detailed explanation of Maxwell's equations using

*Corresponding author Tel. No.: +91-948-061-3804.
Email address: shivaramktshiv@gmail.com (K. T. Shivaram)

the finite element method (FEM), and Zaglmayr [2] described the importance and use of higher-order FEM for electromagnetic field computation. Solving eigenvalue problems remains a central challenge in computational electromagnetics. Recent studies have addressed related electromagnetic and energy applications, including permanent-magnet generators [3], solar thermoelectric power systems [4], thermoelectric annular couplings [5], and switched-reluctance motor optimization [6].

Planar eigenanalysis has been considered by Trefethen and Betcke [7], while multiply connected domain problems have been studied by Chen *et al.* [8]. Other related work includes eigenvalue and eigenfunction calculations for the Laplace operator [9], two-dimensional waveguide problems [10], microfluidic-channel modelling in planar waveguides [11], and eigenvalue analysis of elastic structures [12]. The computation and study of eigenvalues for complicated curved domains is important for particle-accelerator structures [13] and for acoustic problems in bounded geometries [14]. For simple geometries, such as balls and rectangular spaces, explicit formulas may exist; however, intricate curved geometries require numerical methods.

Several methods have been adapted for these problems, including the null-field boundary integral equation (BIE) method, the Burton–Miller method, the boundary element method (BEM), finite differences, and conventional FEMs [15]. Boundary integral equations, point-matching methods, and singular-value decomposition techniques have also been used. For multiply connected domains, however, some approaches may produce spurious eigenvalues [16, 17]. Finite element analysis has therefore become increasingly important as computational capacity has improved. Mesh generation is an essential prerequisite for FEM and many related applications. Most mesh-generation tools use triangular elements; however, lower-order triangular meshes may limit accuracy for complex problems. Higher-order finite elements can improve numerical accuracy using a relatively coarse mesh, but the generation of high-quality unstructured curvilinear meshes remains challenging.

The excellent accuracy and low diffusion and dispersion errors of higher-order FEM make it suitable for electromagnetic applications. Nevertheless, standard higher-order FEM is not often used for electromagnetic problems because the Jacobian may lose sparsity as the element order increases, which can increase processing time and memory requirements. Difficulties in mesh optimization, mesh creation, and finite element computation also restrict its use. This paper addresses these issues by providing an efficient higher-order FEM together with an automated Four-node, Eight-node, and Twelve-node quadrilateral mesh generator in MAPLE-18 for arbitrarily curved domains. The formulation is motivated by the need for accurate and efficient computational eigensolvers in energy and electromagnetic applications. It uses a finite element algorithm, a suitable discretization strategy, and an appropriate quadrature rule to compute numerical solutions of the Helmholtz equation for curved geometries.

Several examples are used to demonstrate the validity of the proposed method. Section 2 presents the mathematical formulation and mesh automation for quadrilateral meshes with Four-node, Eight-node, and Twelve-node. Section 3 describes the eigenvalue calculation for planar and multiply connected regions. Section 4 explains the FEM model for the Helmholtz equation. Section 5 presents the numerical results and comparisons with existing solutions.

Table 1: Mesh parameters for the targeted experimental architectures.

No.	Domain Geometry	Elements		Nodes	
		Case 1[a]	Case 2[b]	Case 1[a]	Case 2[b]
1	Circular domain	166	504	664	2016
2	Square removed from circular domain	240	960	960	3840
3	Union of two circular domains	240	960	960	3840
4	Circular region, two unequal holes	249	996	996	3984
5	L-shaped domain, curved border	996	1464	3984	5856

Note: [a]Case 1 denotes the initial/coarser mesh configuration; [b]Case 2 denotes the subsequent refined/finer mesh configuration.

Table 2: Eigenvalues of waveguide 1.

Eigenvalues (E)	Ref. [18]	4-noded mesh	8-noded mesh	12-noded mesh
E_1	6.24606	6.25150	6.24533	6.24605
E_2	6.39316	6.39775	6.39031	6.39310
E_3	6.39316	6.39671	6.39655	6.39212
E_4	6.81384	6.85443	6.81422	6.81386
E_5	6.81384	6.83106	6.81990	6.81375
E_6	7.45774	7.58874	7.45331	7.45703

Table 3: Eigenvalues of waveguide 2.

Eigenvalues (E)	Ref. [19]	4-noded mesh	8-noded mesh	12-noded mesh
E_1	2.19	2.18665	2.18996	2.19100
E_2	2.33	2.34800	2.34285	2.33451
E_3	2.33	2.33763	2.33653	2.33579
E_4	2.67	2.67709	2.67715	2.67735
E_5	2.76	2.75991	2.76028	2.76001

Table 4: Eigenvalues of waveguide 3.

Eigenvalues (E)	Ref. [20]	4-noded mesh	8-noded mesh	12-noded mesh
E_1	1.00000	1.13773	1.06634	1.00028
E_2	1.77629	1.85609	1.71138	1.77563
E_3	3.19074	3.28804	3.18335	3.19141
E_4	3.19074	3.28845	3.14774	3.19744

Table 5: Eigenvalues of waveguide 4.

Eigenvalues (E)	Ref. [21]	4-noded mesh	8-noded mesh	12-noded mesh
E_1	4.86	4.90532	4.88174	4.86866
E_2	4.86	4.92060	4.87007	4.86615
E_3	6.78	6.79115	6.78554	6.78019
E_4	6.78	6.84430	6.78313	6.78578
E_5	7.89	7.90019	7.89935	7.89648

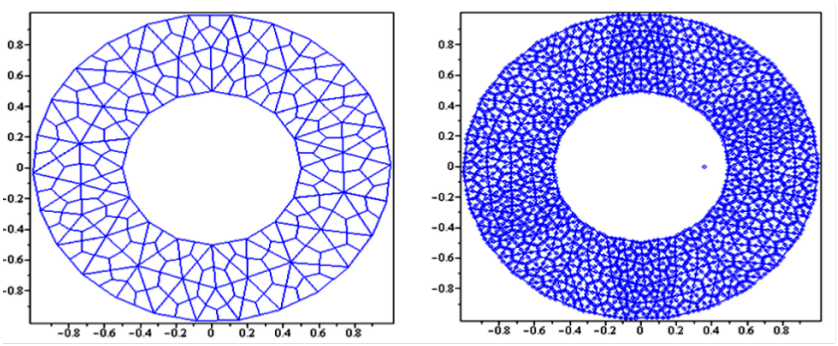

(a)

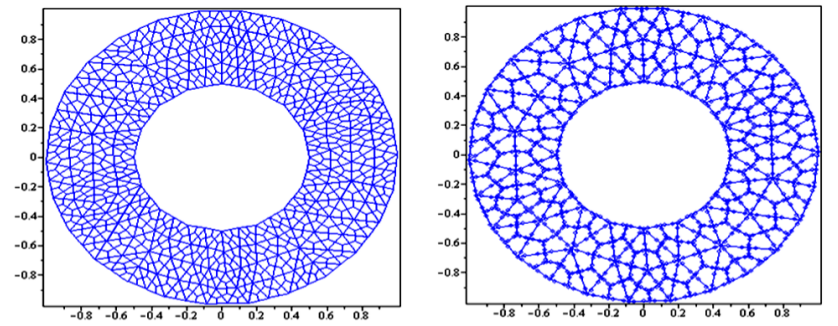

(b)

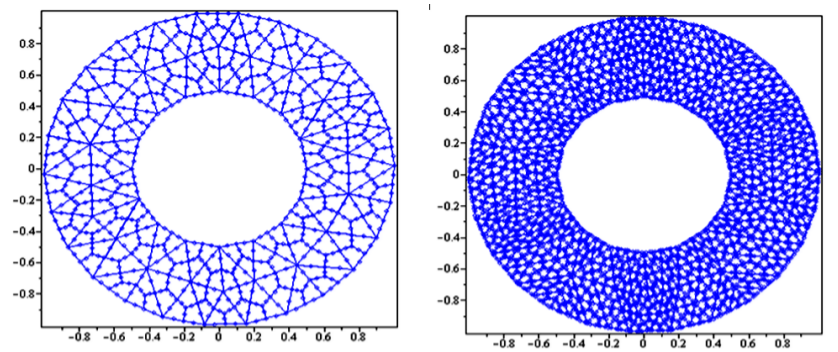

(c)

Figure 1: A circular domain with quadrilateral meshes of Four-node, Eight-node, and Twelve-node with 166 and 504 elements.

Table 6: Eigenvalues of waveguide 5.

Eigenvalues (E)	Ref. [22]	4-noded mesh	8-noded mesh	12-noded mesh
E_1	7.0202	7.13035	7.09540	7.02934
E_2	13.7866	14.0788	13.8774	13.7822
E_3	18.1018	18.3149	18.1702	18.1054
E_4	25.2249	25.4359	25.3385	25.2250
E_5	28.8085	28.9905	28.8213	28.8088
E_6	34.8575	34.9427	34.8855	34.8883

2. Mesh formulation and automation

In finite element analysis, interpolation functions are used to describe how a field variable varies within an element in terms of its nodal values. Following Ref. [23], this relationship is written as

$$U = \sum_{i=1}^{((n+2)(n+1))/2} N_l^n(\xi_1, \xi_2)\, u_l^e. \tag{1}$$

Here, u is the element field variable at any point, u_l^e represents the nodal value of u, and N_l^n denotes the triangular shape function of order n at node l. The standard triangle is a right-angled isosceles triangle with unit side length. Each triangle is split into quadrilaterals with Four-node, Eight-node, and Twelve-node. Lagrange interpolation functions for two-dimensional elements can be obtained by multiplying one-dimensional Lagrange interpolation functions. Thus, the two-dimensional Lagrange shape functions are represented by $N_l(x, y)$, with

$$N_l(\xi_1, \xi_2) = L_l(\xi_1) L_l(\xi_2). \tag{2}$$

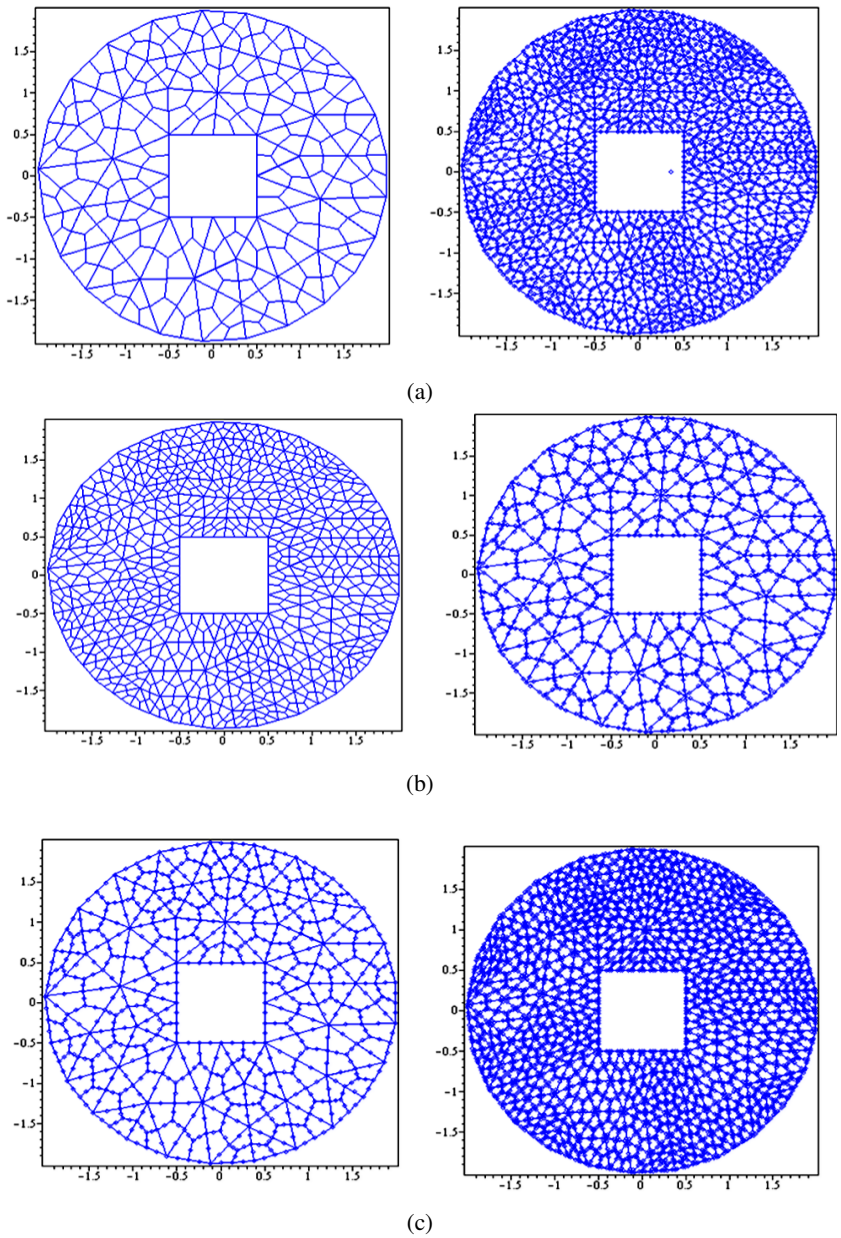

Figure 2: Quadrilateral meshes with Four-node, Eight-node, and Twelve-node for a circular domain with a square removed, with 240 and 960 elements.

The Galerkin weighted-residual finite element method is used to transform the governing equation for Four-node, Eight-node, and Twelve-node quadrilateral elements and the Jacobian, as described by Rathod & Karim [24]. The proposed approach automatically converts triangular elements into quadrilateral elements by adding midside nodes. This procedure reduces the computational effort required to evaluate numerical integrals in the finite element formulation. In the standard pattern, each isolated triangle is split into three quadrilaterals by joining the midside nodes with straight lines.

The same procedure is applied to each triangle in the domain so that complex domains with curved edges are fully discretized into quadrilaterals with Four-node, Eight-node, and Twelve-node while preserving mesh conformity. The method refines the problem domain and produces meshes whose elements conform to the desired geometry. The mesh-generation scheme developed in this paper is integrated into MAPLE-18 programs. The automated mesh-creation processes for Four-node, Eight-node, and Twelve-node elements allow finite element analysis to be performed efficiently. As the mesh density increases, the time needed to generate and reconstruct the model also increases. However, quadrilateral mesh-model development is generally faster than triangular mesh-model development because a triangular mesh contains more elements and therefore requires more calculations.

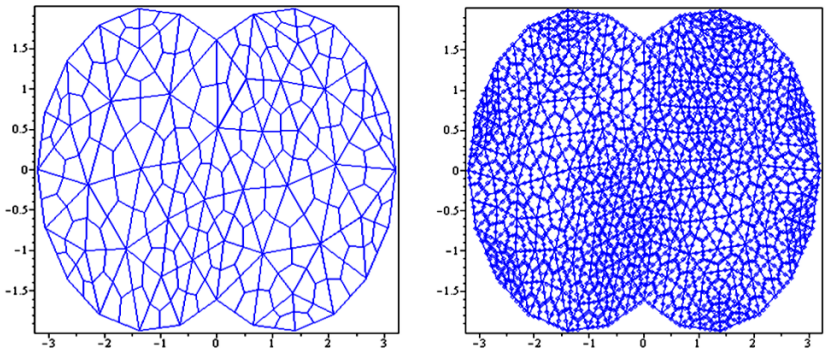

(a)

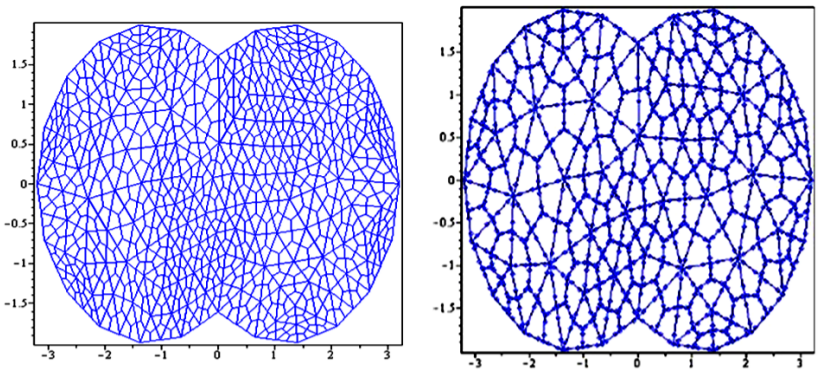

(b)

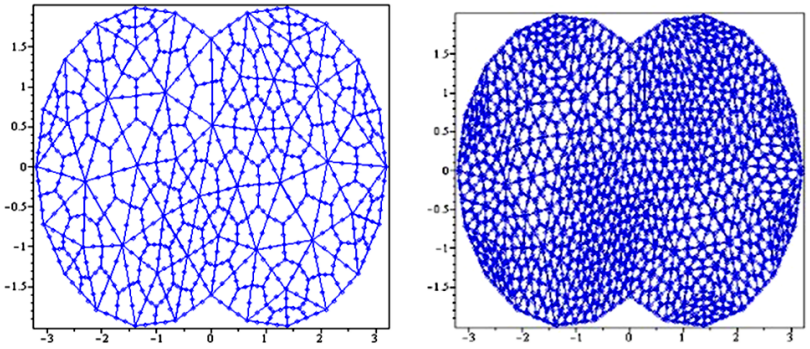

(c)

Figure 3: Two circular disk domains joined using quadrilateral meshes with Four-node, Eight-node, and Twelve-node with 240 and 960 elements.

3. Eigenvalue calculation for planar and multiply connected areas

This section evaluates the suitability and reliability of the proposed optimal Galerkin FEM method. Five waveguide test problems are considered for computing eigenvalues in energy-related applications. The method is used to solve eigenproblems governed by the Helmholtz equation over curved geometries, including planar and multiply connected domains.

3.1. Waveguide 1

The first example is an annular domain with outer and inner circular radii $a = 1$ and $b = 0.5$, respectively. Figure 1 shows the domain with 166 and 504 quadrilateral elements for Four-node, Eight-node, and Twelve-node elements. The numerical results in Ref. [18, 25] were calculated using the BEM with the classical BIE and NDBIE approaches. That study showed that both methods can accurately determine true eigenvalues. The proposed discretization method uses 166 Four-node, Eight-node, and Twelve-node quadrilateral elements to confirm convergence to the true eigenvalues.

3.2. Waveguide 2

The second domain is a square removed from a circle, with an exterior circular boundary and an interior square boundary.

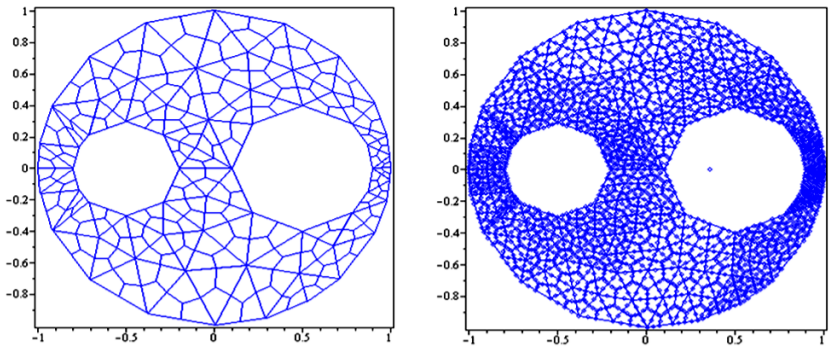

(a)

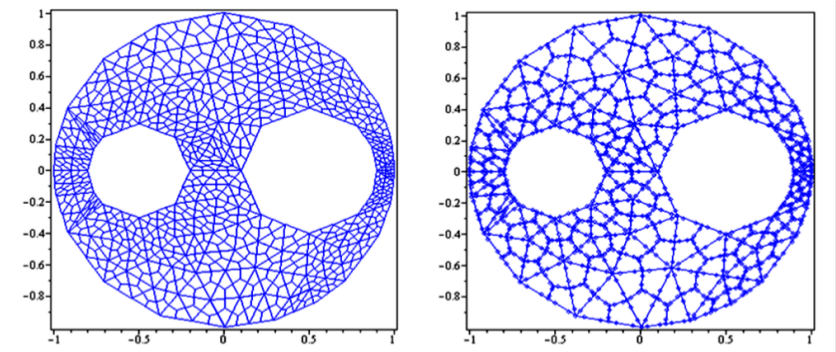

(b)

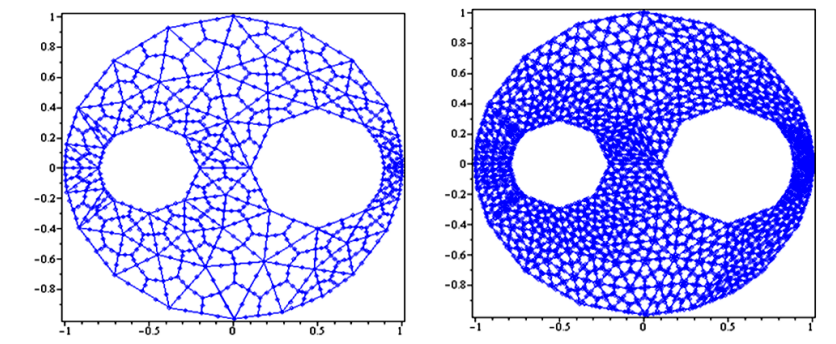

(c)

Figure 4: Quadrilateral meshes with Four-node, Eight-node, and Twelve-node creating a circular region with two unequal holes with 249 and 996 elements.

Such domains occur in acoustic problems. Figure 2 shows the domain discretized using 240 and 960 quadrilateral elements with Four-node, Eight-node, and Twelve-node. Numerical solutions for this eigenvalue problem are evaluated for these domains, and the first ten eigenvalues obtained using FEM and BEM are reported in Ref. [19, 26].

3.3. Waveguide 3

Figure 3 shows the union of two planar circular disk domains, each with centers at ±1.1913 and a radius of 2.002. The domain is discretized into 240 and 960 quadrilateral elements with Four-node, Eight-node, and Twelve-node. The numerical solutions are compared with the results in Ref. [20, 27].

3.4. Waveguide 4

In this example, the boundaries consist of an exterior circle with radius $r = 1$ and eccentricity $e = 0.5$, together with two interior circles of radii $r = 0.3$ and $r = 0.4$. Figure 4 shows the domain discretization for two cases using 249 and 996 quadrilateral elements with Four-node, Eight-node, and Twelve-node. The numerical solutions are compared with the results in Zienkiewicz et al. [27].

3.5. Waveguide 5

The fifth domain is a curved L-shaped region obtained from two squares by removing a unit circle, resulting in a quarter-circular curved boundary. This domain is related to the Sinai billiard, a well-known example in chaotic dynamics. Figure 5

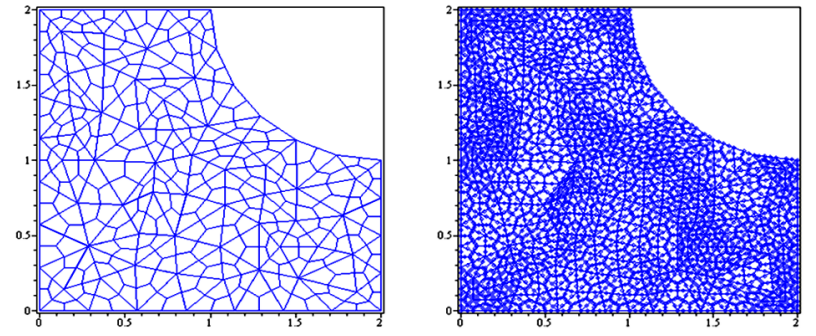

(a)

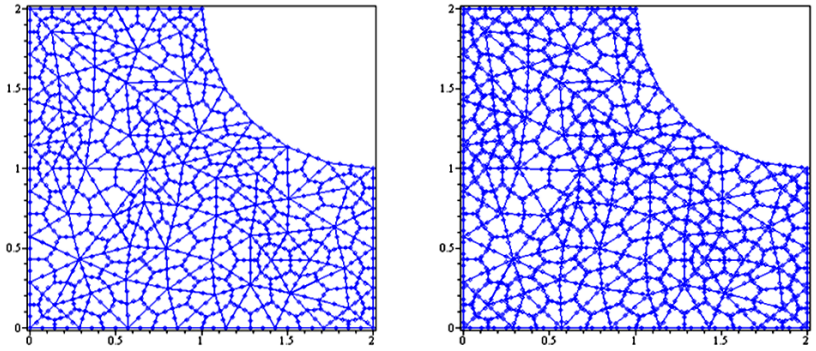

(b)

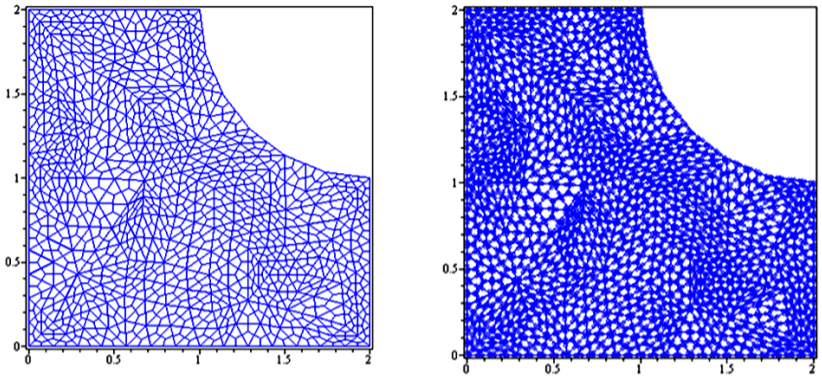

(c)

Figure 5: L-shaped domain with a quarter-circular curved boundary, quadrilateral meshes with 3984 and 5856 nodes with 996 and 1464 elements.

shows the discretization of the domain into two cases using 996 and 1464 Four-node, Eight-node, and Twelve-node quadrilateral elements. The eigenvalues for this problem are compared with numerical solutions reported in Ref. [27].

4. FEM model for the Helmholtz equation

Electromagnetic processes in generators, transformers, and motors convert mechanical energy into electrical energy and vice versa. PDEs provide mathematical formulations for these physical systems, and accurate numerical solutions are needed to predict electromagnetic-system behaviour. The Helmholtz equation for electromagnetic wave propagation in arbitrary waveguides is first discretized using FEM and the proposed Four-node, Eight-node, and Twelve-node meshes. Depending on wave type and geometry, waveguides may be circular, L-shaped, ridge-shaped, coaxial, or rectangular. The cutoff frequencies of waveguides are important for microwave applications and require reliable computational methods. Previous studies have obtained cutoff wavenumbers for transverse electric (TE) and transverse magnetic (TM) modes in waveguides with arbitrary cross-sections using several methods [22, 27].

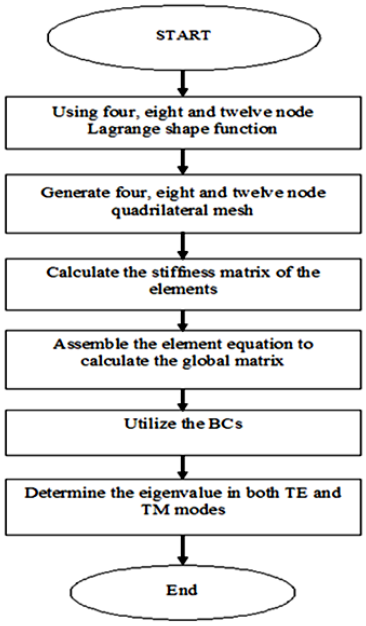

Figure 6: Diagrammatic flowchart for automating the FEM to calculate the eigenvalue of an arbitrary waveguide.

The Helmholtz equation for a waveguide can be written as

$$-\nabla^2\phi + \sigma^2\phi = 0, \tag{3}$$

where ϕ is the wave amplitude and σ is the cutoff wavenumber. For TM modes, the wave amplitude vanishes at the boundary, whereas for TE modes the normal derivative is zero at the boundary.

The Galerkin weighted-residual finite element method is used to transform the waveguide-domain element geometry into Lagrange shape functions for circular domains, circular domains with a square removed, domains with two circular disks removed, circular regions with two unequal holes, and L-shaped waveguides with a quarter-circular curved boundary. The resulting algebraic system is

$$[K + R]\,\phi = F. \tag{4}$$

Here, K and R are stiffness matrices, and ϕ is the displacement vector. The matrix K is expressed as

$$\begin{aligned} K_{i_1 i_2} &= \iint_{\omega_e} \frac{\partial N_{i_1}}{\partial x}\frac{\partial N_{i_2}}{\partial x}\,dx\,dy + \iint_{\omega_e} \frac{\partial N_{i_1}}{\partial y}\frac{\partial N_{i_2}}{\partial y}\,dx\,dy \\ &= K_{xx}^{(i_1,i_2)} + K_{yy}^{(i_1,i_2)}. \end{aligned} \tag{5}$$

In this expression, ω_e represents the area of an element, N_{i_1} and N_{i_2} are Lagrange shape functions, and $i_1, i_2 = 1, 2, \ldots, N$. The terms $K_{xx}^{(i_1,i_2)}$ and $K_{yy}^{(i_1,i_2)}$ are determined from

$$\begin{aligned} K_{xx}^{(i_1,i_2)} = \int_{-1}^{1}\int_{-1}^{1} &\left(\frac{\partial N_{i_1}}{\partial\alpha}\frac{\partial x}{\partial\beta} - \frac{\partial N_{i_1}}{\partial\beta}\frac{\partial x}{\partial\alpha}\right) \\ &\times\left(\frac{\partial N_{i_2}}{\partial\alpha}\frac{\partial x}{\partial\beta} - \frac{\partial N_{i_2}}{\partial\beta}\frac{\partial x}{\partial\alpha}\right)\frac{1}{J}\,d\alpha\,d\beta, \end{aligned} \tag{6}$$

and

$$\begin{aligned} K_{yy}^{(i_1,i_2)} = \int_{-1}^{1}\int_{-1}^{1} &\left(-\frac{\partial N_{i_1}}{\partial\alpha}\frac{\partial y}{\partial\beta} + \frac{\partial N_{i_1}}{\partial\beta}\frac{\partial y}{\partial\alpha}\right) \\ &\times\left(-\frac{\partial N_{i_2}}{\partial\alpha}\frac{\partial y}{\partial\beta} + \frac{\partial N_{i_2}}{\partial\beta}\frac{\partial y}{\partial\alpha}\right)\frac{1}{J}\,d\alpha\,d\beta, \end{aligned} \tag{7}$$

where

$$J = \frac{\partial(x,y)}{\partial(\alpha,\beta)} = \frac{\partial x}{\partial\alpha}\frac{\partial y}{\partial\beta} - \frac{\partial x}{\partial\beta}\frac{\partial y}{\partial\alpha}. \tag{8}$$

The matrix R is given by

$$R = \int_{\omega_e} \sigma^2\, N_{i_1}\, N_{i_2}\,dx\,dy. \tag{9}$$

Using the Gauss quadrature rule for quadrilaterals of order $N = 5$, the matrix components K and R are obtained for each element. Each quadrilateral element is then assembled into a global matrix equation using the global node numbering. After applying the boundary conditions, the modified Helmholtz equation is reduced to an eigenvalue problem. The eigenvalues are computed to determine the TM modes, and the lowest value is identified as the cutoff wavenumber. Figure 6 summarizes the automated higher-order finite element procedure for calculating eigenvalues for arbitrary waveguide cross-sections.

The procedures described in Section 2 can therefore be used to compute Helmholtz-equation eigenvalues by FEM. The proposed method combines optimal quadrature points with an efficient discretization strategy to reduce error in finite element evaluation and to improve the reliability of the computational procedure.

5. Numerical results

The effectiveness of the proposed meshing technique is confirmed by comparing mesh characteristics and computational requirements across different geometries and mesh configurations. The meshing system is implemented in MAPLE for two-dimensional geometries using uniform and non-uniform Four-node, Eight-node, and Twelve-node quadrilateral elements. Multiple domains with different mesh widths and element orders are considered to show how these factors affect the number of nodes, number of elements, and computational time.

Example 1

Higher-order quadrilateral elements with Four-node, Eight-node, and Twelve-node provide improved performance over lower-order triangular elements in electromagnetic simulations. The automated higher-order meshing approach reduces computational time, degrees of freedom, and element count. Table 2 presents the numerical results obtained for this example and compares them with Ref. [7, 27], demonstrating the accuracy of the approach for determining cutoff wavenumbers in region 1. Here, E_1 denotes the first eigenvalue and E_6 denotes the sixth eigenvalue.

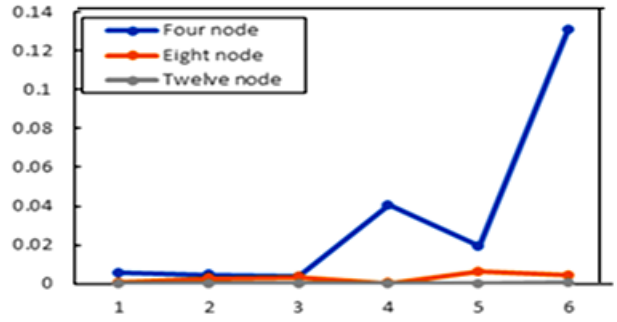

(a)

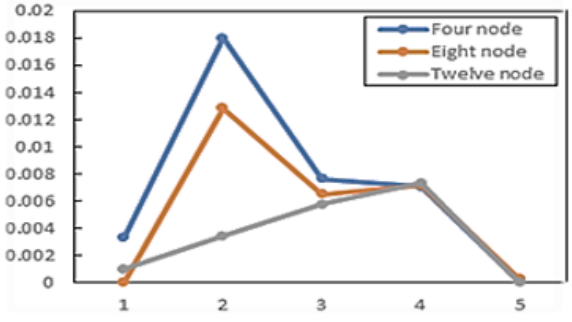

(b)

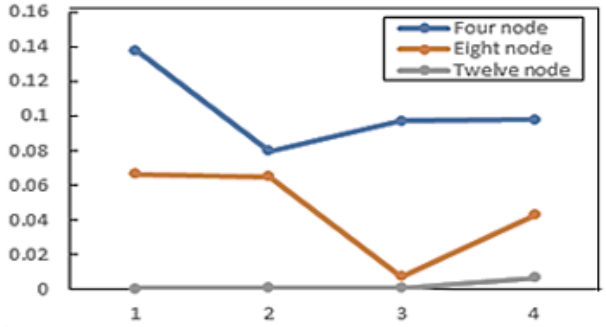

(c)

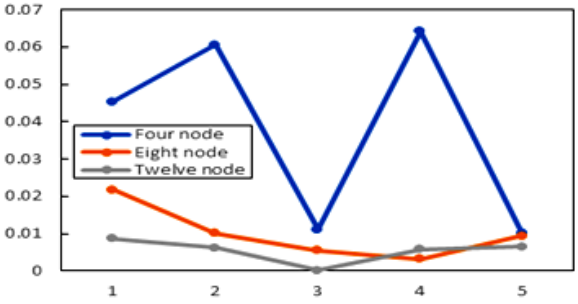

(d)

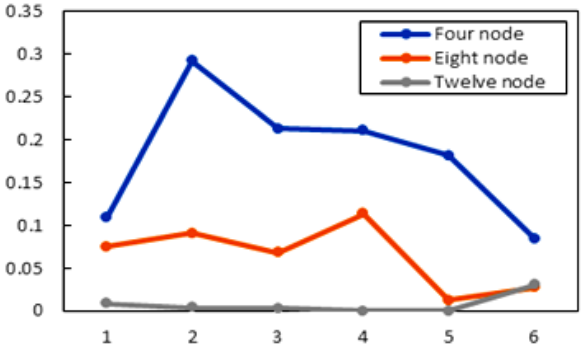

(e)

Figure 7: Absolute error profiles comparing the present method with existing formulations in the literature across the targeted experimental architectures: (a) waveguide 1 metrics; (b) waveguide 2 metrics; (c) waveguide 3 metrics; (d) waveguide 4 metrics; and (e) waveguide 5 metrics based on numerical configurations in Refs. [18–22].

Example 2

The second domain is a square cut out of a circle, as shown in Figure 2. The domain discretization using quadrilateral elements with Four-node, Eight-node, and Twelve-node is summarized in Table 3. The first ten eigenvalues calculated using FEM and BEM are listed in Refs. [7, 27]. The proposed method is used to calculate the first five eigenvalues, which are compared with the numerical solutions in Refs. [7, 28].

Example 3

Figure 3 shows the union of two planar circular disk domains, and Table 4 summarizes the domain discretization using quadrilateral elements with Four-node, Eight-node, and Twelve-node. The proposed approach is used to determine the first four eigenvalues, and the results are compared with the numerical solutions in Ref. [27].

Example 4

For the circular domain with two unequal holes shown in Figure 4, the eigenvalues are calculated using the proposed method. The discretization with quadrilateral elements having Four-node, Eight-node, and Twelve-node is summarized in Table 5. The first five eigenvalues are compared with the numerical solutions in Ref. [7, 27].

Example 5

The fifth domain is the curved L-shaped region shown in Figure 5. Its discretization using quadrilateral elements with Four-node, Eight-node, and Twelve-node is summarized in Table 6. The proposed method is used to compute the first six eigenvalues, which are compared with the numerical solutions reported in Ref. [7, 27].

Eigenvalue analysis techniques for acoustic and electromagnetic applications have become increasingly important. The present work is intended to support wider use of automated meshing schemes combined with FEM for such eigenvalue problems. In the higher-order case, the number of Gauss quadrature points needed to calculate the element stiffness matrix is reduced. A higher-order FEM is therefore proposed for computing eigenvalues in curved geometries using automated higher-order mesh generators. The method is fully implemented in MAPLE-18, and the examples demonstrate its performance. For each case, the mesh density is increased until the numerical solution reaches the desired accuracy. The results show that the accuracy achieved in Ref. [28] required approximately 5000 triangular elements, whereas the proposed Four-node, Eight-node, and Twelve-node quadrilateral elements require about 166 to 1464 quadrilateral elements in the examples considered. Thus, the quadrilateral-element formulation can reduce computational complexity. With $N = 5$ in the Gauss quadrature rule, the absolute errors between the present numerical solutions and the reference solutions [7, 25, 28] are shown in Figure 7. Increasing the order N may further improve convergence.

6. Conclusion

This study presents a fully developed quadrilateral finite element mesh-generation approach with Four-node, Eight-node, and Twelve-node for complex domains with curved boundaries in energy-related applications. The aim is to automate the finite element approach so that efficient and accurate numerical solutions can be obtained for several energy and electromagnetic problems. The proposed higher-order finite element approach provides a practical method for estimating eigenvalues in curved structures. The numerical results show that the method provides accurate solutions of Helmholtz-equation eigenvalue problems in curved geometries by combining an efficient finite element formulation, an effective discretization technique, and an appropriate quadrature rule. The approach may also be useful for applications involving semiconductor films, photonic crystals, anisotropic slabs, and quantum electronics.

Data availability

The authors will provide the data for this study upon reasonable request.

Declaration of competing interest

The authors declare that they have no known competing financial interests or personal relationships that could have appeared to influence the work reported in this manuscript.

Funding

This research received no specific grant from any funding agency in the public, commercial, or not-for-profit sectors.

References

[1] A. Bondeson, T. Rylander & P. Ingelstrom, *Computational electromagnetics*, Springer, New York, USA, 2005, pp. 87–151. https://doi.org/10.1007/0-387-29150-1.

[2] S. Zaglmayr, *High order finite element methods for electromagnetic field computation*, Ph.D. dissertation, Institute for numerical mathematics, Johannes Kepler University, Altenberger Strasse, Austria, 2006. Available online: https://www.numerik.math.tugraz.at/~zaglmayr/pub/szthesis.pdf.

[3] E. Kurt, H. Gor & M. Demirtas, "Theoretical and experimental analyses of a single phase permanent magnet generator (PMG) with multiple cores having axial and radial directed fluxes", Energy conversion and management **77** (2014) 163. https://doi.org/10.1016/j.enconman.2013.09.013.

[4] Z. G. Shen, S. Y. Wu, L. Xiao & Z. Chen, "Proposal and assessment of a solar thermoelectric generation system characterized by a fresnel lens, cavity receiver and heat pipe", Energy **141** (2017) 215. https://doi.org/10.1016/j.energy.2017.09.051.

[5] Z. G. Shen, S. Y. Wu & L. Xiao, "Assessment of the performance of annular thermoelectric couples under constant heat flux condition", Energy conversion and management **150** (2017) 704. https://doi.org/10.1016/j.enconman.2017.08.058.

[6] M. J. Navardi, B. Babaghorbani & A. Ketabi, "Efficiency improvement and torque ripple minimization of switched reluctance motor using FEM and seeker optimization algorithms", Energy conversion and management **78** (2014) 237. https://doi.org/10.1016/j.enconman.2013.11.001.

[7] L. N. Trefethen & T. Betcke, "Computed eigenmodes of planar regions", Contemporary mathematics **412** (2006) 297. https://people.maths.ox.ac.uk/trefethen/publication/PDF/2006_116.pdf.

[8] J. T. Chen, L. W. Liu & S. W. Chyuan, "Acoustic eigenanalysis for multiply-connected problems using dual boundary element method", Communications in numerical methods in engineering **20** (2004) 419. https://doi.org/10.1002/cnm.679.

[9] E. Akhmetgaliyev, O. P. Bruno & N. A. Nigam, "Boundary integral algorithm for the Laplace Dirichlet-Neumann mixed eigenvalue problem", Journal of computational physics **298** (2015) 1. https://doi.org/10.1016/j.jcp.2015.06.009.

[10] R. Misawa, K. Niino & N. Nishimura, "A fast multipole method (FMM) for waveguide problems of 2-D Helmholtz equation and its application to eigenvalue problems", Wave motion **63** (2016) 1. https://doi.org/10.1016/j.wavemoti.2015.12.006.

[11] K. Asha, N. K. Suryanarayana, K. Narayan & P. K. Pattnaik, "Design and modeling of microfluidic channel in a dielectric planar waveguide using COMSOL multiphysics", in *Emerging research in computing, information, communication and applications*, Springer, New Delhi, India, 2016, pp. 79-87. https://doi.org/10.1007/978-81-322-2553-9_8.

[12] C. J. Zheng, C. Zhang, C. X. Bi, H. F. Gao, L. Du & H. B. Chen, "Coupled FE-BE method for eigenvalue analysis of elastic structures submerged in an infinite fluid domain", International journal for numerical methods in engineering **110** (2017) 163. https://doi.org/10.1002/nme.5351.

[13] T. Flisgen, U. van Rienen & J. Heller, "Computation of eigenmodes in long and complex accelerating structures by means of concatenation strategies", in *Proceedings of the 5th international particle accelerator conference*, JACoW publishing, Dresden, Germany, 2014, pp. 947–949. https://proceedings.jacow.org/IPAC2014/papers/tuoab01.pdf.

[14] J. S. Alves Carlos & R. S. Antunes Pedro, "The method of fundamental solutions applied to the calculation of eigenfrequencies and eigenmodes of 2D simply connected shapes", Computer modeling in engineering & sciences **2** (2005) 251. https://doi.org/10.3970/cmc.2005.002.251.

[15] J. T. Chen, J. W. Lee, I. L. Chen & P. S. Kuo, "On the null and nonzero fields for true and spurious eigenvalues of annular and confocal elliptical membranes", engineering analysis with boundary elements **37** (2013) 42. https://doi.org/10.1016/j.enganabound.2012.08.005.

[16] J. T. Chen, J. W. Lee, Y. T. Lee & W. C. Lee, "True and spurious eigensolutions of an elliptical membrane by using the nondimensional dynamic influence function method", Journal of vibration and acoustics **136** (2014) 021018. https://doi.org/10.1115/1.4026354.

[17] C. J. Zheng, H. B. Chen, H. F. Gao & L. Du, "Is the Burton-Miller formulation really free of fictitious eigenfrequencies", Engineering analysis with boundary elements **59** (2015) 43. https://doi.org/10.1016/j.enganabound.2015.04.014.

[18] D. V. Griffiths, J. Huang & R. P. Schiermeyer, "Elastic stiffness of straight-sided triangular finite elements by analytical and numerical integration", Communications in numerical methods in engineering **25** (2009) 247. https://doi.org/10.1002/cnm.1124.

[19] K. T. Shivaram & H. R. Jyothi, "Finite element approach for numerical integration over family of eight node linear quadrilateral element for solving Laplace equation", Materials today: proceedings **46** (2021) 4336. https://doi.org/10.1016/j.matpr.2021.03.437.

[20] K. T. Shivaram, L. M. P. Harshitha, H. P. Chethana & K. Nidhi, "Finite element mesh generation technique for numerical computation of cutoff wave numbers in rectangular and l-shaped waveguide", in *Proceedings of the 3rd international conference on inventive computation technologies*, IEEE xplore, Coimbatore, India, 2018, pp. 704–706. https://ieeexplore.ieee.org/document/9034432.

[21] A. M. Yogitha, K. T. Shivaram, S. M. Rajesh & N. Mahesh Kumar, "Numerical computation of cut off wave number in polygonal waveguide by eight node finite element mesh generation approach", Journal of the Nigerian society of physical sciences **6** (2024) 2149. https://doi.org/10.46481/jnsps.2024.2149.

[22] K. Lekhana & K. T. Shivaram, "A method for creating twelve-node finite element meshes to find the cutoff wave number for polygonal and circular waveguides", International journal of basic and applied sciences **14** (2025) 59. https://doi.org/10.14419/y9648s16.

[23] A. M. Yogitha & K. T. Shivaram, "A twelve-noded finite element approximation to 2D-Poisson equations with a dirac line source", Journal of mechanics of continua and mathematical sciences **20** (2025) 26. https://doi.org/10.26782/jmcms.2025.05.00003.

[24] H. T. Rathod & M. S. Karim, "Synthetic division based integration of rational functions of bivariate polynomial numerators with linear denominators over a unit triangle $0 \leq \xi, \eta \leq 1, \xi + \eta \leq 1$ in the local parametric space (ξ, η)", Computer methods in applied mechanics and engineering **181** (2000) 191. https://doi.org/10.1016/S0045-7825(99)00225-6.

[25] C. J. Zheng, C. X. Bi, C. Zhang, Y. B. Zhang & H. B. Chen, "Fictitious eigenfrequencies in the BEM for interior acoustic problems", Engineering analysis with boundary elements **104** (2019) 170. https://doi.org/10.1016/j.enganabound.2019.03.042.

[26] J. T. Chen, J. H. Lin, S. R. Kuo & S. W. Chyuan, "Boundary element analysis for the Helmholtz eigenvalue problems with a multiply connected domain", Proceedings of the royal society of London A: mathematical, physical and engineering sciences **457** (2001) 2521. https://doi.org/10.1098/rspa.2001.0806.

[27] O. C. Zienkiewicz, R. L. Taylor & J. Z. Zhu, *The finite element method: its basis and fundamentals*, 7th ed., Elsevier, 2005, pp. 1-20. https://doi.org/10.1016/B978-1-85617-633-0.00001-0.

[28] J. N. Reddy, *An introduction to the finite element method*, 3rd ed., McGraw-Hill, New York, USA, 2006. ISBN: 0-07-246685-5.